

The differential diagnosis of benign and malignant breast cancer using shear wave elastography (SWE).

Baohua Wang¹, Zhenyu Cai², Ying Hu¹, Jing Wang¹, Yanhua Chu¹, Tian'an Jiang^{1*}, Jing Cheng¹, Shusen Zheng³

¹Department of Ultrasound, the First Affiliated Hospital, College of Medicine, Zhejiang University, Hangzhou, PR China

²Department of Ultrasound, Zhejiang Medical and Health Group Hangzhou Hospital, Hangzhou, P.R. China

³Division of Hepatobiliary and Pancreatic Surgery, Department of Surgery, First Affiliated Hospital, School of Medicine, Zhejiang University, PR China

Abstract

The purpose of our study is to explore the efficiency of Shear Wave Elastography (SWE) in predicting malignancy Breast Cancer (BC). 63 patients with normal mammary glands and 61 patients with invasive carcinoma were detected by Real-time Tissue Elastography (RTE). Two SWE images of breast hyperplasia with fibroadenoma and invasive breast carcinoma were also obtained. For the SWE characteristics, maximum, minimum, mean elasticity and SWE ratio were acquired. The SWE ratio was counted to reflect the stiffness of lesions, and a high ratio demonstrated a stiff lesion. Kruskal-Wallis one-way ANOVA, Receiver Operating Characteristic (ROC) curve, and Z-Test were used for statistical analysis. Our results indicated that SWE in patients with normal mammary glands showed a light-blue coloured lesion and the SWE values (E_{mean}) was 7.1 kPa. SWE in patients with invasive carcinoma revealed a yellow-to-red coloured mass, and the SWE values (E_{mean}) was 243.6 kPa. The cut-off values of the ROC curve analysis at lesion (E_{max}) and gland ratio (E_{rat}) were 55.8 kpa and 3.45. The Z value was 0.915, and the P value was 0.36 for ROC curve between E_{max} and E_{rat} . The SWE value (E_{mean}) in front of the fat layer was 12.6 kPa in patients with breast hyperplasia accompanying fibroadenoma. The SWE values (E_{mean}) in front of the fat layer was 23.9 kPa in patients with invasive carcinoma. Breast cancers with invasive characteristics had high SWE ratios. Therefore, SWE may provide potential application value for predicting prognosis.

Keywords: Shear wave elastography (SWE), Breast cancer, Malignant tumor, Benign tumor, Diagnosis.

Accepted on July 17, 2017

Introduction

Breast Cancer (BC) is identified to be the most common cancer and the principal cause of cancer death among females worldwide [1]. In 2015, cancer was accounting for 429.16 million new cases and 281.42 million deaths in the China, among them, BC accounted of 2.47% in deaths with 69.5 million cases. Despite the enormous progress of novel treatments in recent few decades, the five-year relative survival rates of BC with I, II, III and IV, 5 y survival rate of BC were 80%, 52%, 42% and 14%, respectively [2,3]. The high incidence and poor prognosis of BC are mainly due to the lack of effective measures of diagnosis and treatment, and patients are often at advanced stages when are diagnosed [1,4]. The current therapies for patients who suffered from BC are mainly including chemotherapy and radiotherapy, with very limited therapeutic efficacy and even along with several unexpected side effects [5-7]. Therefore, it is particularly important for the early diagnosis and identification of BC.

Human tissue lesion has a direct relationship with its hardness changes [8]. Palpation have been widely applied in clinical practice, the hardness of palpation is of great significance to the differential diagnosis of benign malignancy. However, palpation is highly dependent on the doctor's subjective experience [9]. It is difficult to detect the deep lesions and early minor lesions. Therefore, it has become the focus of research to assess the hardness of the lesion objectively in recent years. At present, many methods of elastography are available on many current ultrasound systems. While individual images can be interpreted consistently, it can be difficult to capture the same information across acquisitions or users, and this may hamper clinical utility [10-12].

Real-time Shear Wave Elastography (SWE, Supersonic Imagine, Aix-en-Provence, France) serves as an acoustic pressure wave which contains slow-moving lateral waves, and the speed of the shear wave is related to the square root of the tissue's elastic modulus [13]. Shear wave is spread more

slowly in soft tissues and faster in hard tissues. Ultrafast™ imaging can detect the small changes according to the different stiffness of tissues. Therefore, Real-time SWE is a real-time, reliable, and reproducible manner to make physicians to visualize and quantify the stiffness of tissues. Above all, real-time SWE has lots of advantages, such as real-time guidance using two-dimensional image; The visual display using color elastic image; The repeatability and safety operation and the quantitative analysis using the absolute value of Young's modulus. Therefore, the elastic modulus value of breast solid lesions is of great significance in the evaluation and differential diagnosis of benign and malignant breast solid lesions. Contrasted with the other elastic modulus value, the E_{ratio} and the E_{max} have greater diagnostic value.

In our study, patients with normal mammary glands, invasive carcinoma, breast hyperplasia with fibroadenoma, and invasive breast carcinoma were detected by Real-time Tissue Elastography (RTE), and the maximum, minimum, mean elasticity and SWE ratio were acquired. We then analyzed the E_{mean} value in patients with normal mammary glands before and after 40 y of age. In patients with BC, we drew the ROC curves of E_{max} and E_{ratio} , and concluded the critical values both them to identify its value in terms of disease diagnosis.

Materials and Methods

Participants

The study was approved by the Ethics committee of the Hospital. Each patient has provided the informed consent before enrolment. We chose 63 patients that have mammary glands of ultrasound without exception, and 63 breast lesions including 23 malignant lesions and 40 benign lesions.

All patients were scanned using the Aixplorer ultrasound system (SuperSonic Imagine, Aix-en-Provence, France) in the Hospital between 2013 and 2016. 63 patients had been scheduled for US-guided core biopsy or surgical excision. The features of sonographic images including lesion's shape, margin, echo, height/width, halo, acoustic shadow, flow, which were classified according to the American College of Radiology (ACR) Breast Imaging Reporting and Data System (BI-RADS). All SWE pictures were freely provided to participants.

Inclusion and exclusion criteria

According to the medical records and breast ultrasound, we established the inclusion criteria. We included women with a breast mass revealed with palpation, mammography.

We excluded women with breast implants and those who were pregnant or lactating, who were receiving chemotherapy or radiation therapy for any cancer, who had a history of ipsilateral breast surgery, or who were unwilling or unable to provide informed consent were excluded. Women who have skin lesions and lesions that had been biopsied previously were also excluded.

SWE examination

In our study, all investigators major in BC diagnosis independently accomplished at least 150 breast ultrasound examinations in a year. All participants have accepted the breast ultrasound with breast ultrasound system. On the basis of the ultrasonic breast mass BI-RADS taxonomy made by the radiological society of the United States in 2003 (American College of Radiology, ACR), we chose breast masses of BIRADS classification for 3, 4a, 4b, 4c and 5 classes [14]. Qualified participants will receive additional B-mode ultrasound examination with the ultrasound system (RUBI, Supersonic Imagine, Aix-en-Provence, France), and B-mode characteristics were recorded. After the completion of all identification, SWE was performed with the frequency probe at 4-15 MHz and then we acquired three separate images in SWE mode. According to the shape of the breast masses, the entire lesion area was covered as far as possible, and then the Q-BOXTM function was started to measure the E_{max} , E_{mean} , E_{sd} values. We then selected the hardest area of the diseased tissues (2 mm × 2 mm, circular region) and normal breast tissues at the same depth (2 mm × 2 mm, circular region), and then used Q-BOXTM function to detect the ratio of E_{max} . Investigators will evaluate the three qualitatively similar images, and analyze the quantitative SWE characteristics of the mass. Investigators will also carry out a blinded evaluation for the static images of all masses.

Statistical analysis

The continuous variables in this study were dichotomized (for example, normal breast tissues were dichotomized into before and after 40 y old. BC patients were dichotomized into patients with benign tumors and patients with malignant tumors. Lesions were dichotomized into malignant lesions and benign lesions). The significance of differences was assessed using the Chi-square test. The quantitative values maximum elasticity (E_{max}), median elasticity ratio (E_{rat}), median mean elasticity value (E_{mean}), and minimum elasticity (E_{min}) were collected on SWE. SWE, B-mode, and clinical characteristics were counted statistically between benign and malignant lesions using a Student's t-test or Kruskal-Wallis one-way ANOVA. The Receiver Operating Characteristic (ROC) curve was also drawn, the area under the ROC curve (Area under Curve, AUC) was calculated, and the optimal critical value of diagnosis was obtained, the sensitivity and specificity were calculated. The data were analyzed using IBM SPSS 21 (IBM, Portsmouth, UK). The area under the ROC curve for The SWE™ (E_{max} and E_{rat}) was analyzed by Z-test. The statistical significance was set at $P < 0.05$.

Results

Two shear wave elastography (SWE™) images of normal breast and invasive carcinoma

SWE imaging technology was firstly used to carry out elasticity quantitative study on normal breast tissue and find the hardness range of normal breast tissue so as to provide the

basis for the further abnormal disease diagnosis. We chose 63 patients that have mammary glands of ultrasound without exception. 63 patients were divided into two groups according to age before and after 40 y of age. Then 63 patients with normal mammary glands were detected by Real-time Tissue Elastography (RTE). As shown in Table 1, the median mean elasticity values (E_{mean}) were 10.925 ± 4.354 and 12.683 ± 4.335 in 63 patients with normal mammary glands before and after 40 y of age ($t=0.169$, $P=0.866$), and the glandular section thickness (cm) were 0.979 ± 0.290 and 0.964 ± 0.386 in 63 patients with normal mammary glands before and after 40 y of age ($t=-1.596$, $P=0.116$). The images of all patients were very similar. As shown in Figure 1 (Top), the results indicated that SWE showed a light-blue coloured lesion, and the SWE values (E_{mean} , E_{min} , E_{max} and E_{sd}) were 7.1 kPa, 5.5 kPa, 9.3 kPa and 0.7 kPa. B-mode image (Bottom) showed an ill-defined, hypoechoic mass.

Table 1. The median mean elasticity value (E_{mean}) of normal breast tissues before and after 40 y of age.

| Data | ≤ 40 (n=28) | >40 (n=35) | t value | P value |
|----------------------------------|----------------|----------------|---------|---------|
| E_{mean} (kpa) | 10.925 ± 4.354 | 12.683 ± 4.335 | ± 0.169 | 0.866 |
| Glandular section thickness (cm) | 0.979 ± 0.290 | 0.964 ± 0.386 | -1.596 | 0.116 |

Table 2. The pathological situation of 66 breast cancer patients.

| Patients with malignant tumors | The number of lesions (N) | Patients with benign tumors | The number of lesions (N) |
|--------------------------------|---------------------------|-----------------------------|---------------------------|
| Invasive carcinoma | 15 | Fibroadenoma | 18 |
| Intraductal carcinoma | 6 | Breast hyperplasia | 12 |
| Pre-invasive carcinoma | 2 | Intraductal papilloma | 2 |
| | | Other | 8 |
| Total | 23 | | 40 |

Table 3. The elastic mould values in benign tumors and malignant tumors.

| Variable | Benign tumors (n=40) | Malignant tumors (n=23) | t value | P value |
|---------------------------------------|----------------------|-------------------------|---------|---------|
| Lesion (E_{max}) | 20.973 ± 7.308 | 82.259 ± 41.370 | -7.042 | <0.01 |
| Gland ratio (E_{rat}) | 1.588 ± 0.543 | 5.260 ± 2.190 | -7.902 | <0.01 |
| Surrounding parenchyma (E_{mean}) | 10.956 ± 3.737 | 15.639 ± 5.607 | -3.575 | <0.01 |

* E_{max} =Maximum elasticity; E_{rat} =Median elasticity ratio; E_{mean} =Median mean elasticity value.

Table 4. The diagnosis of ROC curve according to the cut off points ($E_{max}=55.8$ kpa).

| Lesion (E_{max}) | Patients with malignant tumors | Patients with benign tumors | Total |
|----------------------|--------------------------------|-----------------------------|-------|
| Malignant lesions | 21 | 2 | 23 |
| Benign lesions | 2 | 38 | 40 |

* E_{mean} =median mean elasticity value.

The 63 breast lesions in our study cohort were 23 malignant lesions and 40 benign lesions. 23 malignant lesions included invasive carcinoma (n=15), intraductal carcinoma (n=6), preinvasive carcinoma (n=2); 40 benign lesions included fibroadenoma (n=18), breast hyperplasia (n=12), intraductal papilloma (n=2), and other (n=8) (Table 2).

61 patients with invasive carcinoma were measured by RTE. The images of all patients were very similar. As shown in Figure 1 (Below), the results revealed a yellow-to-red coloured mass. The red showed the highest stiffness and the blue showed the lowest stiffness, and the SWE values (E_{mean} , E_{min} , E_{max} , E_{sd} and E_{rat}) were 243.6 kPa, 161.8 kPa, 298.1 kPa, 40.8 kPa, and 72.4 kPa. B-mode image (Bottom) revealed an ill-defined, hypoechoic mass.

According to statistics, the lesion (E_{max}) in benign tumors (n=40) and malignant tumors (n=23) were 20.973 ± 7.308 and 82.259 ± 41.370 ($t=-7.042$, $P<0.01$). The gland ratio (E_{rat}) in benign tumors (n=40) and malignant tumors (n=23) were 1.588 ± 0.543 and 5.260 ± 2.190 ($t=-7.902$, $P<0.01$).

The surrounding parenchyma (E_{mean}) in benign tumors (n=40) and malignant tumors (n=23) were 10.956 ± 3.737 and 15.639 ± 5.607 ($t=-3.575$, $P<0.01$) (Table 3).

| | | | |
|-------|----|----|----|
| Total | 23 | 40 | 63 |
|-------|----|----|----|

*E_{max}=maximum elasticity.**Table 5.** The diagnosis of ROC curve according to the cut off points (E_{rat}=3.45 kpa).

| Gland ratio (E _{rat}) | Patients with malignant tumors | Patients with benign tumors | Total |
|---------------------------------|--------------------------------|-----------------------------|-------|
| Malignant lesions | 21 | 3 | 24 |
| Benign lesions | 2 | 37 | 39 |
| Total | 23 | 40 | 63 |

*E_{rat}=Median elasticity ratio.**Table 6.** Diagnostic performance characteristics: Comparison Lesion (E_{max}) and Gland ratio (E_{rat}).

| Diagnosis | Sensitivity | Specificity | Accuracy | Positive predictive value | Negative predictive value |
|---------------------------------|-------------|-------------|----------|---------------------------|---------------------------|
| Lesion (E _{max}) | 0.913 | 0.95 | 0.937 | 0.913 | 0.95 |
| Gland ratio (E _{rat}) | 0.913 | 0.925 | 0.921 | 0.875 | 0.949 |

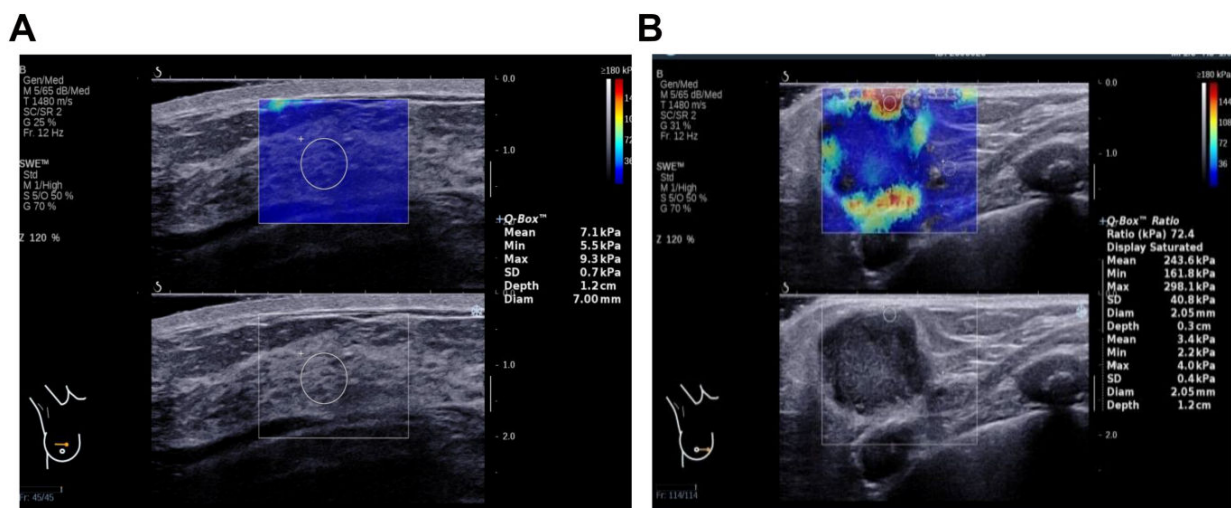
*E_{max}=Maximum elasticity; E_{rat}=Median elasticity ratio.

Figure 1. Two shear wave elastography (SWETM) images of normal breast and invasive carcinoma. (A) 63 patients with normal mammary glands were detected by real-time tissue elastography (RTE). The images of all patients were very similar. SWE (top) showed a light-blue coloured lesion, E_{max} was 9.3 kPa, E_{mean} was 7.1 kPa, E_{min} was 5.5 kPa, E_{sd} was 0.7 kPa. B-mode image (Bottom) showed an ill-defined, hypoechoic mass; (B) 61 patients with invasive carcinoma were measured by RTE. The images of all patients were very similar. SWE (Top) revealed a yellow-to-red coloured mass. The red showed the highest stiffness and the blue showed the lowest stiffness, E_{max} was 298.1 kPa, E_{mean} was 243.6 kPa, E_{min} was 161.8 kPa, E_{sd} was 40.8 kPa, E_{rat} was 72.4. B-mode image (Bottom) revealed an ill-defined, hypoechoic mass. E_{max} indicates maximum elasticity, E_{mean} indicates median mean elasticity value, E_{min} indicates minimum elasticity, E_{sd} indicates standard deviation of elasticity, E_{rat}=median elasticity ratio.

ROC curves for lesion (E_{max})

The cut-off value of the ROC curve analysis at E_{max} was 55.8 kpa, and the area under the receiver operating characteristic curve (AUC) was 0.963 with a sensitivity of 91.3% and specificity of 95.0% (Figure 2). And then the diagnosis of ROC curve was analyzed according to the cut off points (E_{max}=55.8 kpa). The number of malignant lesions was 21, and the number of benign lesions was 2 in patients with malignant tumors (n=23). The number of malignant lesions was 2, and the number of benign lesions was 38 in patients with benign tumors (n=40). The number of total malignant lesions was 23, and the number of total benign lesions was 40 (Table 4). Therefore, when the cut off points for E_{max} was 55.8 kpa, the accuracy was 93.7%, the positive predictive value was 91.3%, and the negative predictive value was 95.0% (Table 6).

ROC curves for gland ratio (E_{rat})

The cut-off value of the ROC curve analysis at E_{rat} was 3.45, and the area under the receiver operating characteristic curve (AUC) was 0.948 with a sensitivity of 91.3% and specificity of 92.5% (Figure 3). Then the diagnosis of ROC curve was analyzed according to the cut off points ($E_{rat}=3.45$). The number of malignant lesions was 21, and the number of benign lesions was 2 in patients with malignant tumors (n=23). The number of malignant lesions was 3, and the number of benign lesions was 37 in patients with benign tumors (n=40).

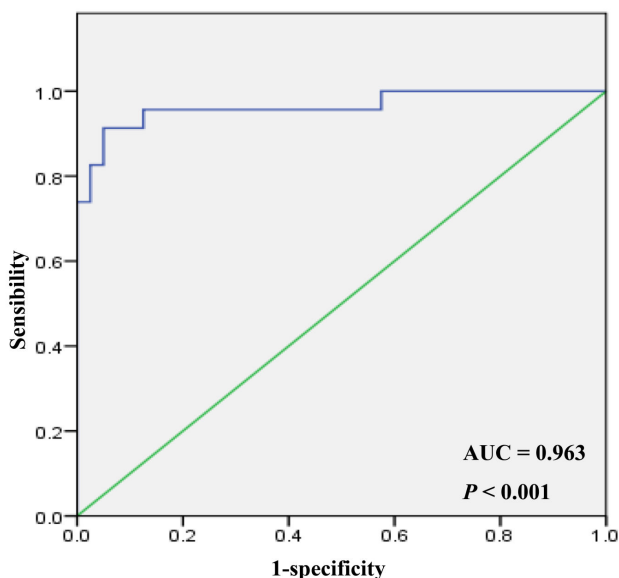


Figure 2. ROC curves for lesion (E_{max}). The chosen cut-off value was 55.8 kpa, the area under the receiver operating characteristic curve (AUC) was 0.963. E_{max} indicates maximum elasticity.

The number of total malignant lesions was 24, and the number of total benign lesions was 39 (Table 5). Therefore, when the cut off points for E_{rat} was 3.45, the accuracy was 92.1%, the positive predictive value was 87.5%, and the negative predictive value was 94.9% (Table 6). ROC curves for lesion (E_{max}) and gland ratio (E_{rat}).

In addition, the area under the ROC curve for The SWETM (E_{max} and E_{rat}) was analyzed by Z-test. The results indicated that the Z value was 0.915, and the P value was 0.36 for ROC curves between lesion (E_{max}) and gland ratio (E_{rat}), suggesting that the diagnostic value of breast lesions diagnosis was high. There was no obvious difference for the area under the ROC curve (Figure 4).

Two SWE images of breast hyperplasia with fibroadenoma and invasive breast carcinoma

Studies revealed that adipose tissues can cause abnormal ultrasonic phenomenon, such as cloudy, fuzzy, etc. When breast lesions infiltrate into subcutaneous fat layer [15,16]. We then detected patients with breast hyperplasia accompanying fibroadenoma using RTE.

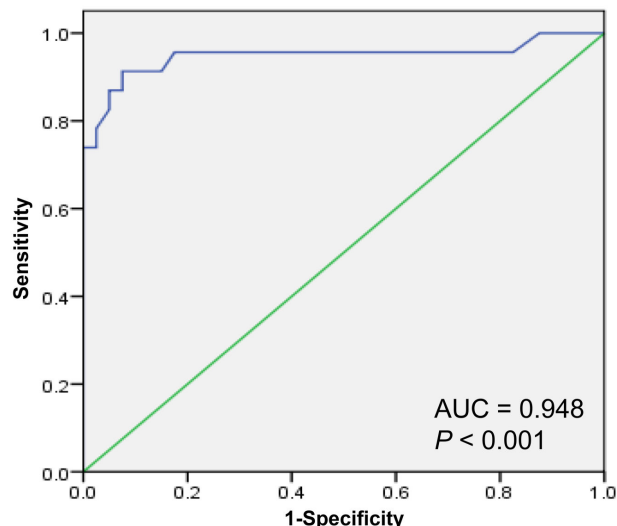


Figure 3. ROC curves for gland ratio (E_{rat}). The chosen cut-off value was 3.45, the area under the receiver operating characteristic curve (AUC) was 0.948. E_{rat} indicates median elasticity ratio.

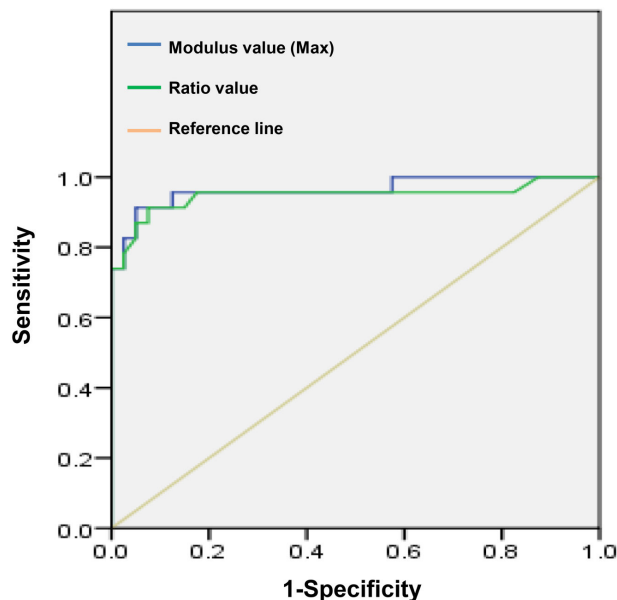


Figure 4. ROC curves for lesion (E_{max}) and gland ratio (E_{rat}). Area under the ROC curve for The SWETM (E_{max} and E_{rat}) was analyzed by Z-test (P value=0.36, Z value=0.915). E_{max} indicates maximum elasticity; E_{rat} indicates median elasticity ratio.

The images of all patients were very similar. As shown in Figure 5 (Top), the results showed that SWE showed a light-blue coloured lesion, and the SWE values in front of the fat layer (E_{mean} , E_{min} , E_{max} , and E_{sd}) were 12.6 kPa, 12.3 kPa, 13.0 kPa, 0.3 kPa.

We also found that the echo change in benign lesions surrounding adipose tissues was that fiber connective tissues were close when local fat was extruded. In addition, patients with invasive carcinoma were measured by RTE.

The images of all patients were very similar. The SWE values in front of the fat layer (E_{mean} , E_{min} , E_{max} , and E_{sd}) were 23.9

kPa, 17.5 kPa, 27.9 kPa, 2.6 kPa. The results also showed the echo changes in malignant lesions surrounding adipose tissues, such as stromal reaction caused by tumor cells; Fibrous tissue hyperplasia in the edge of lesion of subcutaneous tissues with

more fibroblasts, neutral particles, and lymphatic; Direct infiltration of cancer cells in segmental adipose tissues (Figure 5, Below).

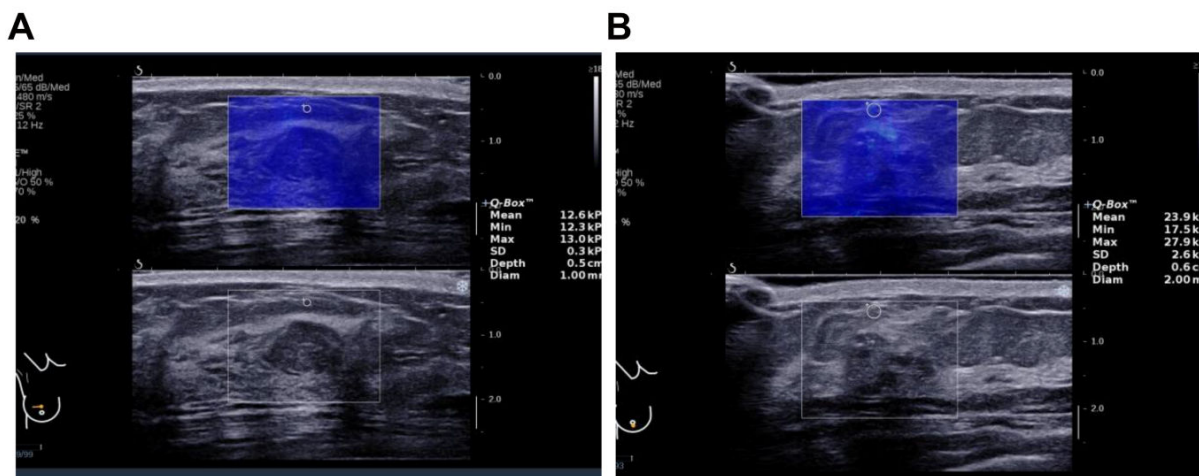


Figure 5. Two SWE images of breast hyperplasia with fibroadenoma and invasive breast carcinoma. (A) Patients with breast hyperplasia accompanying fibroadenoma were detected by RTE. The images of all patients were very similar. SWE values in front of the fat layer were count (E_{max} was 13.0 kPa, E_{mean} was 12.6 kPa, E_{min} was 12.3 kPa, E_{sd} was 0.3 kPa); (B) Patients with invasive carcinoma were measured by RTE. The images of all patients were very similar. SWE values in front of the fat layer were count (E_{max} was 27.9 kPa, E_{mean} was 23.9 kPa, E_{min} was 17.5 kPa, E_{sd} was 2.6 kPa). B-mode image (Bottom) showed an ill-defined, hypoechoic mass.

Discussion

At present, it is an effective method for detection of BC to use breast ultrasound combined breast X-ray examination and other breast imaging method, but its specificity is relatively low [17-19]. Because many benign tumors are relatively soft, malignant tumors are relatively rigid, at the same time, elasticity imaging method can imaging tissue stiffness, so elastography can improve the examination level of patient masses with a low index of suspicion on B-mode ultrasound [20,21]. Many elasticity imaging methods are available on various ultrasound systems, because many of them rely on deformation of tissues, such as strain, the release of pressure, hand pressure, using the breathing exercises or heart movement [10]. However, it's hard to get the same information, which may affect the clinical utility [11,12].

Real-time SWE has been considered to be another useful detection method for the clinical management of patients compared with grayscale ultrasound in benign/malignant differentiation of solid masses [11,12,22]. In addition, stiffness on SWE was also related to tissue signatures, such as tissue grade, size, and nodal stage [23-25]. Therefore, Real-time SWE also can be used to quantitatively analyze the BC tissue stiffness, and provide more abundant information for the diagnosis of breast disease. We aimed to assess the application value of different elastic modulus value using real-time SWE technology in differentiating benign and malignant breast solid lesions.

In our study, we found that SWE in patients with normal mammary glands showed a light-blue coloured lesion. SWE in patients with invasive carcinoma revealed a yellow-to-red

coloured mass. There were statistical significances for the lesion (E_{max}) in benign tumors and malignant tumors; the gland ratio (E_{rat}) in benign tumors and malignant tumors; the surrounding parenchyma (E_{mean}) in benign tumors and malignant tumors. Our results revealed that many types of breast tissues have similar SWE features, lobular cancers have similar stiffness. The variation trend for E_{mean} value was not in conformity with the previous researches in 63 patients with mammary glands before and after 40 y of age. The reasons of discrepancy were that participants are mostly in growth period with concentrated age, and the hormonal changes of participants may affect the changes of breast elastic stiffness. For 61 patients with invasive carcinoma, we found that there were rich blood vessels in malignant lesions around; the tumor epithelial cells were mainly located in the edge area, the infiltrating glands and adipose tissues.

In addition, we found that SWE in patients with breast hyperplasia accompanying fibroadenoma indicated a light-blue coloured lesion with 12.6 kPa E_{mean} . The results also indicated that the echo change in benign lesions surrounding adipose tissues was that fiber connective tissues when local fat was extruded. SWE in patients with invasive carcinoma revealed a yellow-to-red coloured mass with 23.9 kPa E_{mean} . The results also showed that the echo changes in malignant lesions surrounding adipose tissues, such as stromal reaction; fibrous tissue hyperplasia in the edge of lesion of subcutaneous tissues with more fibroblasts; the infiltration of cancer cells in segmental adipose tissues. Therefore, SWE ratios were closely associated with the degree of BC metastasis.

Receiver Operating Characteristic (ROC) analysis is a common graphical analysis technology of classification models [26,27].

ROC analysis is widely used in various fields, such as bioinformatics, medical statistics, radiology, pattern recognition, and machine learning, etc. [28-30]. In addition, some indicators from ROC curve, such as the area under the ROC curve (AUC) has been used as evaluation and construction of classifiers [31,32]. In our study, the chosen cut-off value of E_{\max} was 55.8 kpa. The area under the AUC was 0.963. The chosen cut-off value was E_{rat} 3.45 kpa. The area under the AUC was 0.948. Area under the ROC curve for The SWETM (E_{\max} and E_{rat}) was analyzed by Z-test (P value=0.36, Z value=0.915). The data indicated that the diagnostic values of diagnosis were high both E_{\max} and E_{rat} in breast lesions.

Conclusion

In conclusion, our results indicated that mammary gland can be used as a reference E_{ratio} value; The Z value was 0.915, and the P value was 0.36 for ROC curves between E_{\max} and E_{rat} , indicating that the diagnostic value of breast lesions diagnosis was high; When E_{ratio} value exceeded 3.45 or E_{\max} exceeded 55.8kPa, SWE has higher diagnostic accuracy and specificity. Therefore, real-time SWE can be used to detect the micro vascularization in different lesions, which will provide new clinical information and diagnostic values in benign and malignant lesions.

Acknowledgment

Supported by Education Agency of Zhejiang Province, P. R. China (No. Y201534607) and Health Bureau of Zhejiang Province, P. R. China (No. 2017195594).

Conflict of Interest

None.

References

1. Torre LA, Bray F, Siegel RL, Ferlay J, Lortet-Tieulent J, Jemal A. Global cancer statistics, 2012. *CA Cancer J Clin* 2015; 65: 87-108.
2. Chen W, Zheng R, Baade PD, Zhang S, Zeng H, Bray F, He J. Cancer statistics in China, 2015. *CA Cancer J Clin* 2016; 66: 115-132.
3. Ording AG, Boffetta P, Garne JP, Nystrom PM, Cronin-Fenton D, Froslev T, Lash TL. Relative mortality rates from incident chronic diseases among breast cancer survivors-a 14 year follow-up of five-year survivors diagnosed in Denmark between 1994 and 2007. *Eur J Cancer* 2015; 51: 767-775.
4. French Adjuvant Study Group. Benefit of a high-dose epirubicin regimen in adjuvant chemotherapy for node-positive breast cancer patients with poor prognostic factors: 5-year follow-up results of french adjuvant study group 05 randomized trials. *J Clin Oncol* 2001; 19: 602-611.
5. Burstein HJ, Lacchetti C, Griggs JJ. Adjuvant endocrine therapy for women with hormone receptor-positive breast cancer: American society of clinical oncology clinical practice guideline update on ovarian suppression summary. *J Oncol Pract* 2016; 12: 390-393.
6. Coates AS, Winer EP, Goldhirsch A, Gelber RD, Gnani M, Piccart-Gebhart M, Panel M. Tailoring therapies-improving the management of early breast cancer: St Gallen international expert consensus on the primary therapy of early breast cancer 2015. *Ann Oncol* 2015; 26: 1533-1546.
7. Goldhirsch A, Winer EP, Coates AS, Gelber RD, Piccart-Gebhart M, Thurlimann B, Panel M. Personalizing the treatment of women with early breast cancer: highlights of the St Gallen international expert consensus on the primary therapy of early breast cancer. *Ann Oncol* 2013; 24: 2206-2223.
8. Milly H, Festy F, Andiappan M, Watson TF, Thompson I, Banerjee A. Surface pre-conditioning with bioactive glass air-abrasion can enhance enamel white spot lesion remineralization. *Dent Mater* 2015; 31: 522-533.
9. Zimmermann N, Ohlinger R. Diagnostic value of palpation, mammography, and ultrasonography in the diagnosis of fibroadenoma: impact of breast density, patient age, ultrasonographic size, and palpability. *Ultraschall Med* 2012; 33: 151-157.
10. Itoh A, Ueno E, Tohno E, Kamma H, Takahashi H, Shiina T, Matsumura T. Breast disease: clinical application of US elastography for diagnosis. *Radiol* 2006; 239: 341-350.
11. Chang JM, Moon WK, Cho N, Kim SJ. Breast mass evaluation: factors influencing the quality of US elastography. *Radiol* 2011; 259: 59-64.
12. Chang JM, Moon WK, Cho N, Yi A, Koo HR, Han W, Kim SJ. Clinical application of shear wave elastography (SWE) in the diagnosis of benign and malignant breast diseases. *Breast Cancer Res Treat* 2011; 129: 89-97.
13. Athanasiou A, Tardivon A, Tanter M, Sigal-Zafrani B, Bercoff J, Deffieux T, Neuenschwander S. Breast lesions: quantitative elastography with supersonic shear imaging-preliminary results. *Radiol* 2010; 256: 297-303.
14. Park CS, Lee JH, Yim HW, Kang BJ, Kim HS, Jung JI, Kim SH. Observer agreement using the ACR Breast Imaging Reporting and Data System (BI-RADS)-ultrasound. *Korean J Radiol* 2007; 8: 397-402.
15. Aytakin S, Guder H, Goktay F, Yasar S, Aker F, Aksaray S. Pyoderma gangrenosum and necrotizing fasciitis-like opportunistic invasive cutaneous fungal infection. *Int J Dermatol* 2016; 55: 563-565.
16. Yuan WH, Li AF, Hsu HC, Chou YH. Isolated panniculitis with vasculitis of the male breast suspicious for malignancy on CT and ultrasound: a case report and literature review. *Springerplus* 2014; 3: 642.
17. Berg WA. Supplemental screening sonography in dense breasts. *Radiol Clin North Am* 2004; 42: 845-851.
18. Corsetti V, Ferrari A, Ghirardi M, Bergonzini R, Bellarosa S, Angelini O, Ciatto S. Role of ultrasonography in detecting mammographically occult breast carcinoma in women with dense breasts. *Radiol Med* 2006; 111: 440-448.

19. Houssami N, Irwig L, Simpson JM, McKessar M, Blome S, Noakes J. Sydney breast imaging accuracy study: Comparative sensitivity and specificity of mammography and sonography in young women with symptoms. *Am J Roentgenol* 2003; 180: 935-940.
20. Burnside ES, Hall TJ, Sommer AM, Hesley GK, Sisney GA, Svensson WE, Hangiandreou NJ. Differentiating benign from malignant solid breast masses with US strain imaging. *Radiol* 2007; 245: 401-410.
21. Evans A, Whelehan P, Thomson K, Brauer K, Jordan L, Purdie C, Thompson A. Differentiating benign from malignant solid breast masses: value of shear wave elastography according to lesion stiffness combined with greyscale ultrasound according to BI-RADS classification. *Br J Cancer* 2012; 107: 224-229.
22. Berg WA, Cosgrove DO, Dore CJ, Schafer FK, Svensson WE, Hooley RJ. Shear-wave elastography improves the specificity of breast US: the BE1 multinational study of 939 masses. *Radiol* 2012; 262: 435-449.
23. Evans A, Rauchhaus P, Whelehan P, Thomson K, Purdie CA, Jordan LB, Vinnicombe S. Does shear wave ultrasound independently predict axillary lymph node metastasis in women with invasive breast cancer? *Breast Cancer Res Treat* 2014; 143: 153-157.
24. Xie J, Wu R, Xu HX, Yao MH, Xu G. Relationship between parameters from virtual touch tissue quantification (VTQ) imaging with clinicopathologic prognostic factors in women with invasive ductal breast cancer. *Int J Clin Exp Pathol* 2014; 7: 6644-6652.
25. Youk JH, Gweon HM, Son EJ, Kim JA, Jeong J. Shear-wave elastography of invasive breast cancer: correlation between quantitative mean elasticity value and immunohistochemical profile. *Breast Cancer Res Treat* 2013; 138: 119-126.
26. Lasko TA, Bhagwat JG, Zou KH, Ohno-Machado L. The use of receiver operating characteristic curves in biomedical informatics. *J Biomed Inform* 2005; 38: 404-415.
27. Ogawa W, Nakaya G, Karasawa H. Fitting of ROC curves for continuous data by using correction of the mean and standard deviation. *Nihon Hoshasen Gijutsu Gakkai Zasshi* 2004; 60: 111-117.
28. Liu D, Zhou XH. Semiparametric estimation of the covariate-specific ROC curve in presence of ignorable verification bias. *Biometrics* 2011; 67: 906-916.
29. Yang JY, Dunker A, Liu JS, Qin X, Arabnia HR, Yang W, Yang M. Advances in translational bioinformatics facilitate revealing the landscape of complex disease mechanisms. *BMC Bioinformatics* 2014; 15.
30. Yao W, Li Z, Graubard B I. Estimation of ROC curve with complex survey data. *Stat Med* 2015; 34: 1293-1303.
31. Halligan S, Altman DG, Mallett S. Disadvantages of using the area under the receiver operating characteristic curve to assess imaging tests: a discussion and proposal for an alternative approach. *Eur Radiol* 2015; 25: 932-939.
32. Kottas M, Kuss O, Zapf A. A modified Wald interval for the area under the ROC curve (AUC) in diagnostic case-control studies. *BMC Med Res Methodol* 2014; 14: 26.

***Correspondence to**

Tian'an Jiang
 Department of Ultrasound
 The First Affiliated Hospital
 College of Medicine
 Zhejiang University
 PR China
 E-mail: chenmy@zju.edu.cn